Journal of Alloys and Compounds 518 (2012) 32–37

Contents lists available at SciVerse ScienceDirect

Journal of Alloys and Compounds

journal homepage: www.elsevier.com/locate/jallcom

Effect of Al substitution on magnetocaloric effect in $La_{0.57}Nd_{0.1}Sr_{0.33}Mn_{1-x}Al_xO_3$ ($0.0 \leq x \leq 0.30$) polycrystalline near room temperature

Emna Tka [a,*], Karima Cherif [a], Jemai Dhahri [a], Essebti Dhahri [b], Hafedh Belmabrouk [c], El Kebir Hlil [d]

[a] Unité de Recherche Physique des Solides, Département de Physique, Faculté des Sciences de Monastir, 5019, Université de Monastir, Tunisia
[b] Laboratoire de Physique Appliqué, Faculté des Sciences, B.P. 1171, 3000 Sfax, Université de Sfax, Tunisia
[c] Laboratoire de Micro Electronique, Département de Physique, Faculté des sciences de Monastir, 5019, Université de Monastir, Tunisia
[d] Laboratoire de Cristallographie, CNRS, 25 avenue des Martyrs, B.P. 166, 38042 Grenoble-Cedex 9, France

ARTICLE INFO

Article history:
Received 9 October 2011
Received in revised form
20 December 2011
Accepted 21 December 2011
Available online 29 December 2011

Keywords:
Al doped manganites
Magnetocaloric effect
Magnetic refrigeration
Magnetic entropy change
Relative cooling power

ABSTRACT

We have investigated the effect of aluminum (Al) doping on the magnetic and magnetocaloric properties of $La_{0.57}Nd_{0.1}Sr_{0.33}Mn_{1-x}Al_xO_3$ (LNSMAO) ($0.0 \leq x \leq 0.3$). The Curie temperature T_C of the prepared samples is found to be strongly dependent on the aluminum content and it spans between 238 K and 342 K. It has been analyzed by using two methods: a linear extrapolation of $M(T)$ to zero magnetization and the thermodynamic model. With an increasing Al concentration, a systematic increase in the values of magnetic entropy is observed. The magnitude of the isothermal magnetic entropy ($|\Delta S_M|$) at the FM Curie temperature increases from 2.31 J/kg K for $x = 0$ to a maximum value of 3.58 J/kg K for $x = 0.3$ for a magnetic field change of 10 kOe. Moreover, the relative cooling power (RCP) increases from 23 J/kg to 68 J/kg, respectively. Large magnetic entropy changes upon the application of a low magnetic field and a wide temperature range of T_C suggest that these materials can be used as candidates for magnetic refrigerants.

1. Introduction

Magnetic refrigeration based on the magnetocaloric effect (MCE) has attracted a great deal of interest in the prospect of an energy-efficient and environment-friendly alternative to the common vapor-cycle refrigeration technology in use today [1–3].

Magnetic materials contain two energy reservoirs; the usual phonon excitations connected to the lattice degrees of freedom and magnetic excitations connected to the lattice spin of freedom. These two reservoirs are coupled by the spin–lattice (in other words – magnetoelastic) interactions. An externally applied magnetic field can strongly affect the spin degree of freedom that results in the MCE. Historically, many ferromagnets concerning second-order transition were investigated in an attempt to achieve large magnetocaloric effect (MCE), of which the rare-earth elemental gadolinium Gd was used as a prototypical refrigerant because of near room temperature ferromagnetic transition ($T_C = 293$ K) and a large magnetic entropy change ($|\Delta S_M^{max}| = 13.3$ J/kg K for $\Delta H = 7$ T), due to a high spin value ($S = 5/2$ for Gd) [4].

Nonetheless, because of the high price of Gd (~$4000/kg), its usage as an active magnetic refrigerant (AMR) in magnetic refrigerators is limited. Therefore, the search for a new working substance at low prices and large MCE becomes a main research topic in this field. At present, besides some possible candidates, such as $Gd5(Si_{1-x}Ge_x)_4$ [4], $MnAs_{1-x}Sb_x$ [5], $MnFeP_{1-x}As_x$ [6], $Tb_{1-x}Gd_xAl_2$ [7] and RM_2 (where R = rare earth, M = Al, Co, Ni) [5,8–12], the hole-doped manganites with the general formula $Ln_{1-x}A_xMnO_3$ (Ln = trivalent rare earth, A = divalent alkaline earth) with perovskite structure should be one of the most promising materials because they present numerous advantages such as the low production costs, the ease of shaping and preparation, the tunable T_C and the chemical stability [13].

In this context, several studies have been performed on the effects of the substitution in the Ln-site [14,15], however, only a few studies have been reported in the substitution effects in the Mn-site [16,17] especially the presence of the non-magnetic ion in this Mn-site which influences the magnetotransport, the MR and the MC properties of the material. In fact, it has been revealed that $La_{1-x}Sr_xMnO_3$ based manganite materials, modulated by Mn-site substitution with Cr, Cu, Ni, Co, Fe etc., present a large isothermal entropy change upon an application of a magnetic field around the ordering temperature T_C [18–21].

To gain more insight into this aspect, we have studied the effect of the non-magnetic ion Al^{3+} substituted in the Mn-site on new magnetocaloric material $La_{0.57}Nd_{0.1}Sr_{0.33}MnO_3$ which might has properties applicable at room temperature.

* Corresponding author. Tel.: +216 96205196.
E-mail address: emna_tka@yahoo.fr (E. Tka).

0925-8388/$ – see front matter © 2011 Elsevier B.V. All rights reserved.
doi:10.1016/j.jallcom.2011.12.100

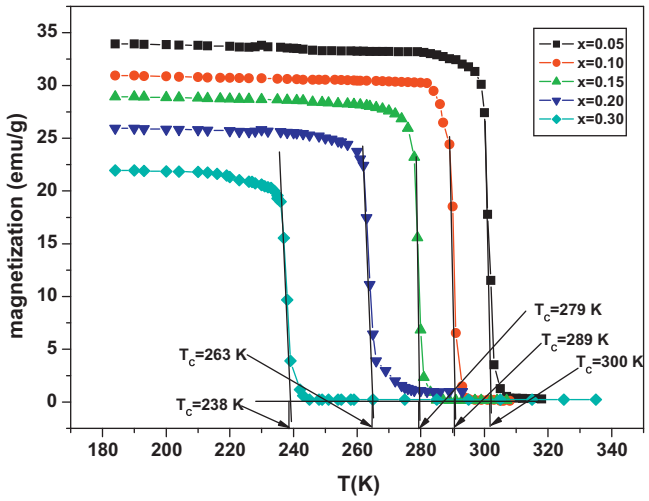

Fig. 1. Variation of the magnetization M vs. temperature for $La_{0.57}Nd_{0.1}Sr_{0.33}Mn_{1-x}Al_xO_3$ samples at 0.05 T for $x = 0.05$, 0.1, 0.15, 0.2 and 0.3.

2. Experimental

Polycrystalline samples of $La_{0.57}Nd_{0.1}Sr_{0.33}Mn_{1-x}Al_xO_3$ ($0.0 \le x \le 0.3$) prepared by conventional solid-state reaction method were taken from the same batches used in a previous work [22]. Room temperature X-ray diffraction measurement showed that the samples are single phase perovskite rhombohedral (space group $R\bar{3}c$) structures. The magnetization (M) vs. temperature (T) and magnetization vs. magnetic field (H) curves were measured by using a Foner magnetometer equipped with a super-conducting coil. Magnetization of the samples was measured in an isothermal regime under an applied magnetic field varying from 0 to 10 kOe. In the vicinity of Curie temperature, isothermal M (H) curves were obtained by steps of 5 and 2 K. The temperature steps were smaller near T_C and larger further away.

3. Results and discussion

3.1. Magnetization investigation

In order to analyze the effect of Al substitution on the Curie temperature, two methods have been used to determine T_C:

(i) The first one is a linear extrapolation of M (T) to zero magnetization. The Curie temperature T_C of the samples defined as the temperature corresponding to the inflection point of the M (T) curve. Fig. 1 shows the temperature dependence of magnetization for the LNSMAO ($0.05 \le x \le 0.30$) samples during cooling and warming measured under $\mu_0 H = 500$ Oe and T_C data extracted by extrapolation are shown in it. The obtained values of Curie temperature T_C are 300, 289, 279, 263 and 238 K, respectively, for $x = 0.05$, 0.10, 0.15, 0.20 and 0.30.

(ii) The second method is based on the thermodynamic model: Amaral et al. [23,24] discussed the magnetic properties of manganites in terms of the Landau theory of phase transitions. Here, the magnetic energy MH has been included in the expression of Gibb's free energy as given by:

$$F(T, M) = F_0 + \frac{1}{2}AM^2 + \frac{1}{4}BM^4 - MH$$

where A and B, known as Landau coefficients, depend both on pressure P and temperature T and provide information about magnetoelastic coupling and electron–electron interaction [23–26]. The last term in the equation describes the energy of spins which is expected to be slowly varying with temperature. On the other hand, the coefficient A shows negative and positive values below and above T_C respectively.

By assuming equilibrium condition of Gibb's free energy: $(\delta F/\delta M) = 0$, the magnetic equation of state is obtained as: $AM + BM^3 = H$. In this equation, M is the experimentally measured mass magnetization and equal to $M_S + M_i$, where M_S is the spontaneous and M_i is the true magnetization caused by the application of the field H.

Thus, by plotting the experimental data in the form, $A + BM^2 = H/M$, the temperature dependence of the parameters A and B can be extracted, from which the transition point T_C and the temperature dependence of M_S below T_C can be determined.

In order to gain a deeper understanding of the magnetic properties and to confirm the ferromagnetic behavior at low temperatures, we plotted the magnetization vs. the applied magnetic field (from 0 to 10 kOe) obtained at various temperatures for the LNSMAO samples ($x = 0.05$ and 0.20) in Fig. 2. We have not shown the M (H) data of the other samples since they have a similar behavior. These curves provide evidence of a close relationship between the magnetization M and the applied magnetic field H. Below T_C, the magnetization M increases sharply with magnetic applied field for ($H < 0.5$ kOe) and then saturates above 1 kOe. The saturation magnetization shifts to higher values with decreasing temperature. When the temperature approaches T_C, the magnetization change

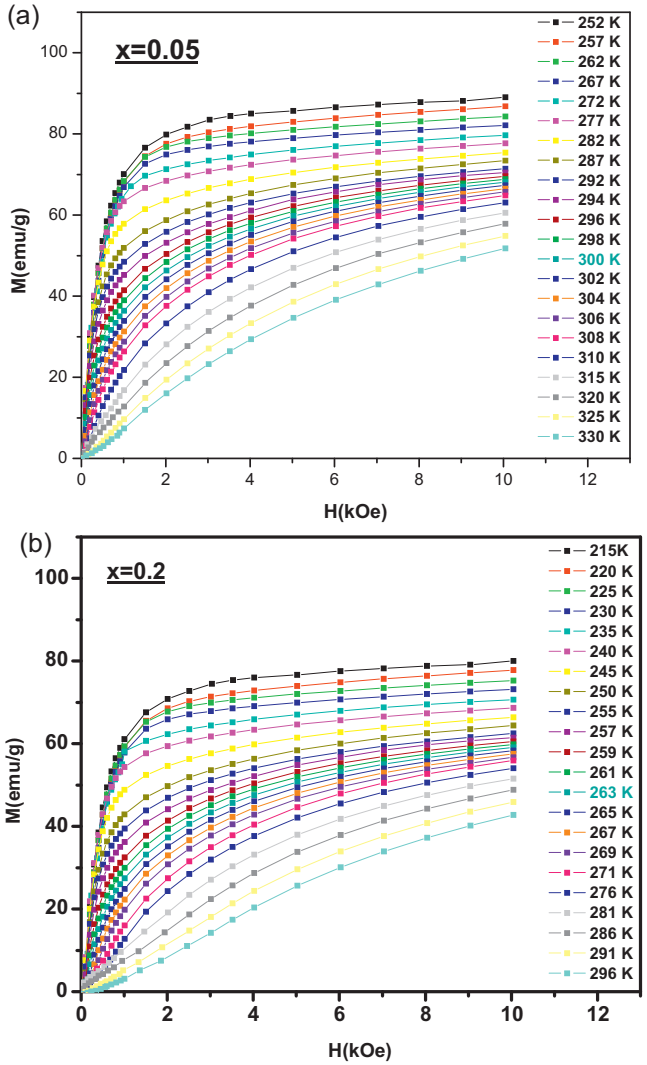

Fig. 2. Isothermal magnetization for $La_{0.57}Nd_{0.1}Sr_{0.33}Mn_{1-x}Al_xO_3$ samples measured at different temperature around T_C for: (a) $x = 0.05$, (b) $x = 0.2$.

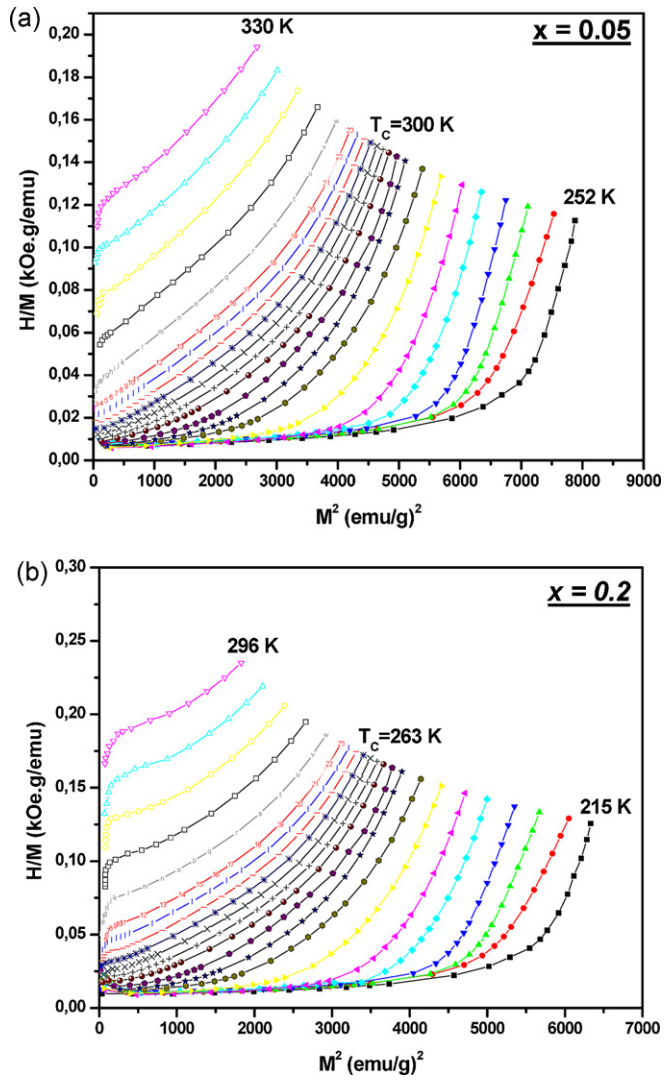

Fig. 3. Arrott curves for $La_{0.57}Nd_{0.1}Sr_{0.33}Mn_{1-x}Al_xO_3$ samples for (a) $x = 0.05$, (b) $x = 0.2$. The temperatures of the isotherms are indicated.

becomes large. This result confirms the ferromagnetic behavior of our samples at low temperatures.

To understand the nature of the magnetic transition of the samples, Arrott plots of H/M vs. M^2 covering a broad temperature range around T_C are plotted in Fig. 3 for $x = 0.05$ and 0.2. According to Banerjee's criterion [27], samples which exhibit second-order phase transition show a positive slope at all points of M^2 in the Arrott plot, at and below T_C. Whereas samples which exhibit first-order phase transition show a negative slope for certain range of M^2 values. Clearly, an inflection point and positive slopes in the high-field regions are observed in Fig. 3, indicating the occurrence of second-order magnetic transition. The temperature dependence of parameters A can be extracted by fitting to the linear section of the transition formed curves (Fig. 4). The Curie temperature T_C is given by $A = A'(T - T_C)$, where A varies from negative to positive values with increasing temperature, and the temperature corresponding to the value where it crosses zero is consistent with the T_C. The values of T_C obtained for the samples LNSMAO ($x = 0.0$, 0.05, 0.10, 0.15, 0.20 and 0.30) are respectively 345, 299, 287, 276, 260 and 234 K. The obtained values of T_C determined by the two methods mentioned above are nearly the same.

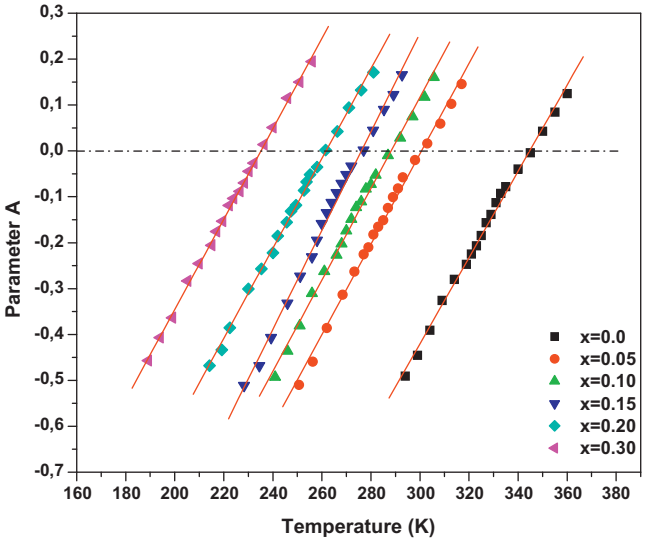

Fig. 4. Parameter (A) as a function of temperature.

3.2. Magnetocaloric effect

The magnetocaloric effect is an intrinsic property of magnetic materials. It is the response of the material to the application or removal of magnetic field, which is maximized when the material is near its magnetic ordering temperature (Curie temperature T_C). A recent study has shown that the substitution of Al for Mn in $La_{0.7}Sr_{0.3}MnO_3$ effectively lowers the ferromagnetic ordering temperature T_C from ~364.5 K to well below 300 K [28]. The Al^{3+} ion is not magnetic and does not possess any 3d electrons; the substitution of Al for Mn causes a sudden break of the ferromagnetic Mn^{3+}—O—Mn^{4+} interactions without any ferromagnetic compensation which could lead to a much stronger decrease in T_C compared to other transition metal substitutions [28]. These compounds are, therefore, suitable for the studies of MCE in the room-temperature region. Furthermore, it would be interesting to see how a dilution of the Mn lattice by a non-magnetic element like aluminum affects the MCE in the manganites systems. So, to examine this effect on the magnetic-entropy change ΔS_M, the temperature and field dependence of the magnetization $M(T, H)$ was utilized.

According to the classical thermodynamic theory, the magnetic entropy change ΔS_M produced by the variation of a magnetic field from 0 to H_{max} is expressed as follows: [29]

$$\Delta S_M(T, H) = S_M(T, H) - S_M(T, 0) = \int_0^{H_{max}} \left(\frac{\delta S}{\delta H}\right)_T dH \quad (1)$$

From the Maxwell's thermodynamic relationship:

$$\left(\frac{\delta S}{\delta H}\right)_T = \left(\frac{\delta M}{\delta T}\right)_H \quad (2)$$

One can obtain the following expression:

$$\Delta S_M(T, H) = S_M(T, H) - S_M(T, 0) = \int_0^{H_{max}} \left(\frac{\delta M}{\delta T}\right)_H dH \quad (3)$$

Here H_{max} is the maximum external field [30].

According to Eq. (3) the maximum magnetic entropy change is obtained at the Curie temperature where the ferromagnetic–paramagnetic phase transition takes place. In general, the magnetic entropy change ΔS_M is often evaluated thanks to two different numerical calculations. The first approximation method is to directly use the measurement of the M–T curve under different applied magnetic fields. In the case of small

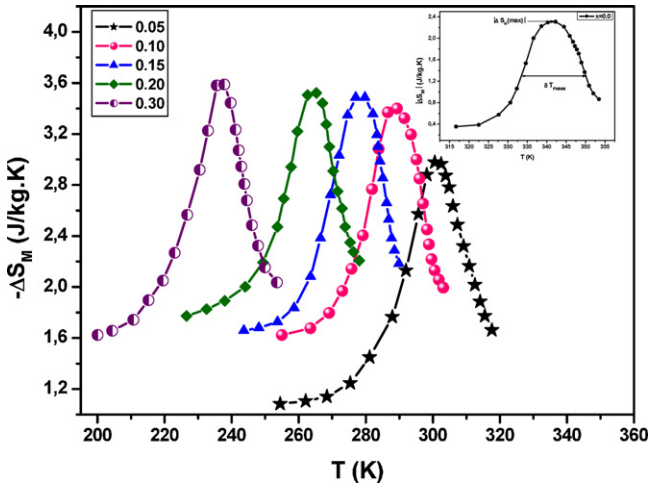

Fig. 5. Magnetic entropy change as a function of temperature of the samples $La_{0.57}Nd_{0.1}Sr_{0.33}Mn_{1-x}Al_xO_3$ for $x = 0.05$, 0.1, 0.15, 0.2 and 0.3. The inset is for $x = 0$.

discrete field ΔH_i, the magnetic entropy change defined in Eq. (1) can be approximated by:

$$\Delta S_M\left(\frac{T_1+T_2}{2}\right) = \left(\frac{1}{T_2-T_1}\right)\left[\int_0^{H_{max}} M(T_2,H)\mu_0 dH - \int_0^{H_{max}} M(T_1,H)\mu_0 dH\right] \quad (4)$$

The ΔS_M values for different ΔH as a function of temperature are presented in Fig. 5. It is clear that the magnetic-entropy change depends on the magnetic field change. The ΔS_M is negative in the entire temperature range for all the samples for $\Delta H = 10$ kOe. However, it increases with lowering temperature from $T \gg T_C$, goes through a maximum around T_C and then decreases for $T \ll T_C$. The magnitude of the peak increases with an increasing value of ΔH for each composition but the peak position is nearly unaffected because of the second order nature of the ferromagnetic transition in these compounds.

As expected, the peak of $-\Delta S_M$ may occur around T_C where the variation in magnetization as a function of temperature is the sharpest [31].

In general, two prerequisites are necessary for inducing large MCE. One is associated with a large enough spontaneous magnetization, while the other is associated with an abrupt drop of magnetization at T_C. Therefore, samples exhibiting the second-order magnetic transition are expected to show a reduced magnetic entropy change and the peak expands with the enhancement of disorder. The maximum isothermal entropy changes for the samples are listed in Table 1. Upon an application of a field 10 kOe for the samples, the largest value of $\Delta S_M \sim 3.58\,J\,kg^{-1}\,K^{-1}$ for the sample with $x = 0.3$ is found at a temperature of 238 K. The large value of $\left|\Delta S_M^{max}\right|$ in LNSMAO may be related to the strong coupling between the spin and the lattice.

Earlier studies have shown that with decreasing the mean radius of B-site $\langle r_B \rangle$, the T_C decreases and results in an enhancement of a spin lattice interaction [32]. As it can be seen from Ref. [22], our investigated samples LNSMAO exhibit a decrease in Mn^{3+}—O^{2-}—Mn^{4+} angle and an increase in Mn—O length. These results lead to a weakening of the double exchange interaction between Mn^{3+} and Mn^{4+} ions and consequently leads to a reduction in both T_C and carrier mobility (right scale of Fig. 6).

What is worth noting is that our results are excellently comparable to those reported by Dhahri et al. [33] where the authors showed that the substitution of Co for Mn in $La_{0.67}Pb_{0.33}Mn_{1-x}Co_xO_3$ compounds leads to an increase in $-\Delta S_M^{max}$ and a decrease in the Curie temperature.

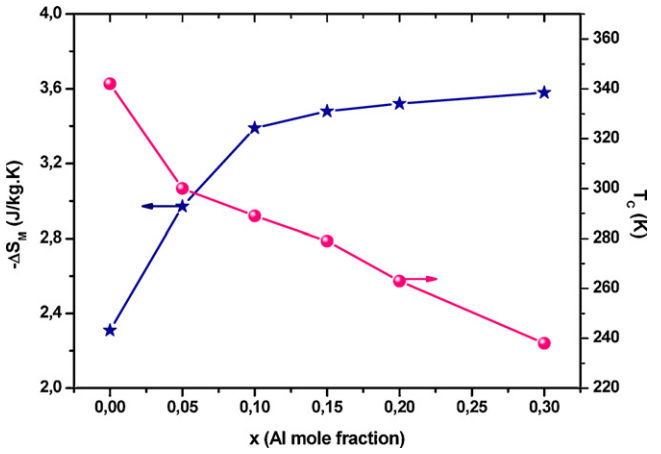

Fig. 6. The dependences of the magnetic entropy change and the Curie temperature (T_C) on the Al-doped concentration (x) for $La_{0.57}Nd_{0.1}Sr_{0.33}Mn_{1-x}Al_xO_3$ ($x = 0$, 0.05, 0.1, 0.15, 0.2 and 0.3).

The maximum value of ΔS_M plotted as a function of composition (x) is shown in Fig. 6 (left scale) which shows gradual increases in $-\Delta S_M^{max}$ values.

The main panel of Fig. 7 presents the magnetic entropy change ΔS_M for LNSMAO ($x = 0.2$) as a function of temperature under different magnetic fields. A remarkable feature is the exact correspondence between the maximal ΔS_M and the recorded PM–FM transition at T_C, while ΔS_M distributes over a relatively wide T range.

The peak of $-\Delta S_M^{max}$ increases with an increasing value of ΔH for each composition but the peak position is nearly unaffected because of the second order nature of the ferromagnetic transition in these compounds.

To assess the applicability of LNSMAO samples for magnetic refrigeration, the $\left|\Delta S_M^{max}\right|$ values determined in the present studies are compared in Table 1 with those reported in literature for several materials having close T_C and considered promising for such application. The large MCEs found in several manganite systems indicates that these manganites are potential for room-temperature AMR (Active Magnetic Regenerator). In the temperature range of 200–375 K, La—Ca—Mn—O_3 manganites exhibit the largest MCE. In particular, Ulyanov et al. [34] recently found

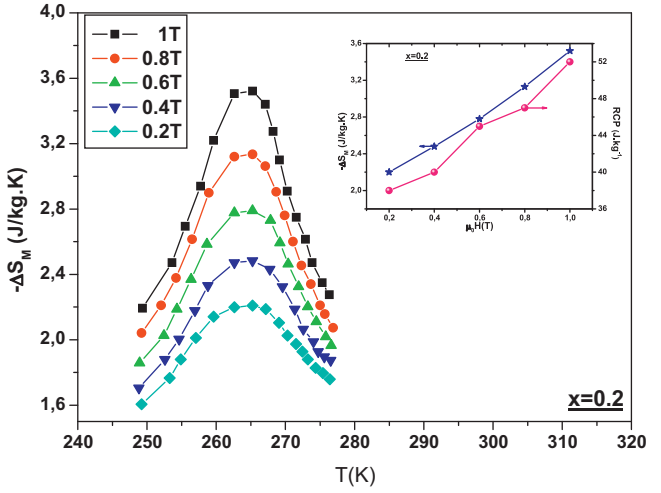

Fig. 7. Temperature dependence of the magnetic-entropy change ΔS_M for different magnetic field intervals for $La_{0.57}Nd_{0.1}Sr_{0.33}Mn_{0.8}Al_{0.2}O_3$ sample. Insert the maximum entropy change $\left|\Delta S_M^{max}\right|$ and the relative cooling power (RCP) values vs. applied magnetic field.

Table 1
The Curie temperature and magnetocaloric parameters of the $La_{0.57}Nd_{0.1}Sr_{0.33}Mn_{1-x}Al_xO_3$ and some important magnetic refrigerant candidate materials.

Sample	T_C (K)	H (kOe)	$\left\|\Delta S_M^{max}\right\|$ (J/kg K)	$\left\|Q_M\,(T_C \pm 10\,K,\quad H = 10\,kOe)\right\|$ (J/kg)	RCP (J/kg)	Refs.
Gd	292	10	3.25	122 ($T_C \pm 25$ K)	–	[33]
$La_{0.57}Nd_{0.1}Sr_{0.33}MnO_3$	342	10	2.31	33	23	This work
$La_{0.57}Nd_{0.1}Sr_{0.33}Mn_{0.95}Al_{0.05}O_3$	300	10	2.97	50.96	40	This work
$La_{0.57}Nd_{0.1}Sr_{0.33}Mn_{0.90}Al_{0.10}O_3$	289	10	3.39	57.57	50	This work
$La_{0.57}Nd_{0.1}Sr_{0.33}Mn_{0.85}Al_{0.15}O_3$	279	10	3.48	59.8	53	This work
$La_{0.57}Nd_{0.1}Sr_{0.33}Mn_{0.80}Al_{0.20}O_3$	263	10	3.52	60.27	59	This work
$La_{0.57}Nd_{0.1}Sr_{0.33}Mn_{0.70}Al_{0.30}O_3$	238	10	3.58	60.8	68	This work
$La_{0.65}Nd_{0.05}Ca_{0.3}Mn_{0.9}Cr_{0.1}O_3$	225	10	0.96	–	98	[40]
$La_{2/3}\,(Ca_{0.95}Sr_{0.05})_{1/3}\,MnO_3$	275	10	3.26	–	71	[41]
$La_{0.7}Sr_{0.3}Mn_{0.9}Al_{0.1}O_3$	310	10	0.61	–	51	[28]
$La_{0.7}Sr_{0.3}Mn_{0.95}Ti_{0.05}O_3$	308	10	9.45	–	42	[28]
$La_{0.67}Pb_{0.33}Mn_{0.7}Co_{0.3}O_3$	260	10	3.22	45.87	63	[33]
$La_{0.67}Ba_{0.33}Mn_{0.95}Fe_{0.05}O_3$	271	10	0.62	–	50	[39]
$La_{2/3}Sr_{1/3}MnO_3$	370	10	1.5	–	41	[41]

$\Delta S_M = 6.25$ J/kg K for $\Delta H = 10$ kOe in a $La_{0.7}Ca_{0.3}MnO_3$ manganite exceeds that of Gd ($\Delta S_M = 3.25$ J/kg K for $\Delta H = 10$ kOe). Compared with Gd and other candidate materials, perovskite materials are more convenient to prepare and exhibit a higher chemical stability as well as a higher resistivity that are favorable for lowering eddy current heating. In addition, they show a much smaller thermal and field hysteresis then any rare-earth and 3d-transtion metal-based alloys.

The MCE peak temperature can be easily tuned in the wide temperature range of 100–375 K, which is beneficial for AMR at various temperatures. Additionally, the manganite materials are the cheapest (~$10/kg) among the existing magnetic refrigerants. These superior features make them more promising for future MR technology.

The results obtained for LNSMAO system over a wide temperature range around the room temperature make this system very useful as a magnetic refrigerant for room temperature magnetic refrigerator because of: a well-defined transition temperature due to a sharp shape of $\left|\Delta S_M\right|(T)$ curve, a modest magnetic entropy change upon application/removal of a low magnetic field and easily controllable magnetic entropy, a good chemical stability and with a quite high efficiency, and ultimately the possibility of being manufactured at a low price.

From our study it is obvious that the perovskites are polycrystalline. A large value of entropy change could be expected in single crystalline samples. Perovskites are easy to prepare and exhibit a higher chemical stability as well as a higher resistivity that are favorable for lowering eddy current heating. Besides, since the Curie temperature of perovskite manganites is doping dependent, a large entropy change could be turned from low temperatures to near and above room temperature, which is beneficial to operating magnetic refrigeration at various temperatures. The large magnetic entropy change in our samples must be originated from the considerable variation of magnetization near T_C. Moreover, it provides insight into the role of the spin–lattice coupling in the magnetic ordering process.

In this context, it is worth comparing the magnetocaloric effects of Al and other B-site dopants like Cr, Co, Ni and Cu in $La_{0.7}Sr_{0.3}Mn_{1-x}M_xO_3$ system. Choudhury et al. [21] studied MCE in $La_{0.7}Sr_{0.3}Mn_{1-x}Ni_xO_3$ ($0 \le x \le 0.05$) and found a maximum entropy change of 3.54 J/kg K under $H = 13.5$ kOe for $x = 0.02$ sample but decreased to 2.33 J/kg K for $x = 0.05$ sample. The T_C of the sample also decreased from 350 K for $x = 0$–320 K for $x = 0.05$. Phan et al. [13] still found higher value of magnetic entropy ($\Delta S_M = 7.65$ J/kg K for $\Delta H = 70$ kOe) in 2% Ni-doped sample. A large magnetocaloric effect ($\Delta S_M = 5.5$ J/kg K for $\Delta H = 10$ kOe) was also found in $La_{0.7}Sr_{0.3}Mn_{0.9}Cu_{0.1}O_3$ [35]. In the series $La_{0.845}Sr_{0.155}Mn_{1-x}M_xO_3$ (M = Mn, Cu, Co), the largest MCE ($\Delta S_M = 2.67$ J/kg K for $\Delta H = 13.5$ kOe) was found for $x = 0.1$% of Cu [36]. All these studies indicate that MCE is enhanced in systems where the spin–lattice interaction is strong at the Curie temperature irrespective of the magnetic nature of the B-site cation as long as the doping level is small. For a higher level doping, when the antiferromagnetic interaction dominates the ferromagnetic double exchange interaction, the magnetic entropy change is reduced.

On the other hand, the magnetic cooling efficiency of refrigerants can be in simple cases, evaluated by considering the magnitude of ΔS_M and its full-width at half-maximum (δT_{FWHM})[37,38]. It is easy to establish the product of the ΔS_M maximum and the full-width at half-maximum ($\delta T_{FWHM} = T_{hot} - T_{cold}$) as RCP $= -\Delta S_M^{max} \times \delta T_{FWHM}$, which stands for the so-called relative cooling power (RCP) to the amount of heat transferred between the cold and the hot sinks in the ideal refrigeration cycle [38]. It is also an important parameter to determine the efficiency of cooling. For the Al doped sample LNSMAO, RCP with $\Delta H = 10$ kOe increases from 23 J/kg for $x = 0$ to 68 J/kg for $x = 0.3$. Nearly similar RCP values have been reported for $La_{0.67}Ba_{0.33}Mn_{1-x}Fe_xO_3$ [39] and $La_{0.7}Sr_{0.3}Mn_{1-x}Al_xO_3$ [28]. Refrigerants with a wide working temperature span and high RCP are in fact very beneficial to magnetic cooling applications. It is worth mentioning that while T_C is largely suppressed, the Al substitution only slightly affects the magnetic cooling effect.

As shown in the inset of Fig. 7 for $x = 0.2$, $\left|\Delta S_M^{max}\right|$ and RCP exhibit an almost linear rise with an increasing field, which is an indication of a much larger entropy change and a relative cooling power to be expected at a higher magnetic field ($\left|\Delta S_M^{max} = 3.52\,J\ kg^{-1}\ K^{-1}\right|$ and RCP = 59 J/kg at 10 kOe), signifying, therefore, the effect of the spin–lattice coupling associated to changes in the magnetic ordering process in the sample.

The heat originated only from magnetic entropy change around ±10 K of T_C, can also be estimated as: $\left|Q_M(T_C \pm 10\,K,\quad H = 10\,kOe)\right| = \int_{T_C-10\,K}^{T_C+10\,K} \Delta S_M(T, H = 10\,kOe)dT$. Q_M the refrigerant capacity obtained at 10 kOe around ±10 K of T_C increases with Al content (Table 1) and is typically found for $x = 0.1$ to be ~47% that of Gd (122.0 J/kg at $T_C \pm 25$ K).

Our results may be interesting enough, compared to materials considered as good for applications in magnetic refrigerators, paving the way for more investigation into materials useful for magnetic refrigeration.

4. Conclusions

In conclusion, we have reported the effects of Al replacement for Mn on the magnetic properties and the MCE in $La_{0.57}Nd_{0.1}Sr_{0.33}Mn_{1-x}Al_xO_3$ for a wide range of Al concentrations ($0.0 \le x \le 0.30$). It has been found that the substitution of Al for Mn results in a decrease in T_C and the saturated magnetization simultaneously. All the samples exhibit a maximum of magnetic entropy

at the phase transition. For the Al substituted series, the magnitude of MCE, the relative cooling power as well as the refrigerant capacity (Q_M) have considerably improved. The $x = 0.3$ composition shows the largest value of magnetic entropy change ($\left|\Delta S_M^{max}\right| = 3.58$ J/kg K at $T_C = 238$ K for $\Delta H = 10$ kOe) in the series and this value is larger than the values reported around the Curie temperature of other half-doped manganites. This compound exhibits a high value of RCP = 68 J/kg. Thanks to their numerous advantages such as the considerable magnetic entropy change, the relative large RCP, and being inexpensive and innocuous raw materials, LNSMAO can be considered as potential magnetic refrigeration materials to be employed in various thermal devices.

References

[1] K.A. Gschneidner Jr., V.K. Pecharsky, A.O. Tsokol, Rep. Prog. Phys. 68 (2005) 1479–1539.
[2] K.A. Gschneidner Jr., V.K. Pecharsky, Annu. Rev. Mater. Sci. 30 (2000) 387–429.
[3] S. Atalay, H. Gencer, V.S. Kolat, J. Non-Cryst. Solids 351 (2005) 2373–2377.
[4] V.K. Pecharsky, K.A. Gschneidner, Phys. Rev. Lett. 78 (1997) 4494–4497.
[5] H. Wada, Y. Tanabe, Appl. Phys. Lett. 79 (2001) 3302–3304.
[6] Q. Tegus, E. Bruck, K.H. Buschow, F.R. de Boer, Nature 415 (2002) 150–152.
[7] F.W. Wang, X.X. Zhang, F.X. Hu, Appl. Phys. Lett. 77 (2000) 1360–1362.
[8] V.K. Pecharsky, K.A. Gschneidner, Appl. Phys. Lett. 70 (1997) 3299–3301.
[9] J.R. Sun, F.X. Hu, B.G. Shen, Phys. Rev. Lett. 85 (2000) 4191.
[10] F.X. Hu, B.G. Shen, J.R. Sun, Z.H. Cheng, G.H. Rao, X.X. Zhang, Appl. Phys. Lett. 78 (2001) 3675–3677.
[11] D.H. Wang, S.L. Tang, H.D. Liu, W.L. Gao, Y.W. Du, Intermetallics 10 (2002) 819–821.
[12] S. Yu. Dan'kov, A.M. Tishin, V.K. Pecharsky, K.A. Gschneidner Jr., Phys. Rev. B 57 (1998) 3478–3490.
[13] M.H. Phan, S.C. Yu, J. Magn. Magn. Mater. 308 (2007) 325–340.
[14] A.M. Aliev, A.G. Gamzatov, A.B. Batdalov, A.S. Mankevich, I.E. Korsakov, Physica B 406 (2011) 885–889.
[15] S.K. Barik, R. Mahendiran, J. Appl. Phys. 107 (2010) 093906–093912.
[16] C. Krishnamoorthi, S.K. Barik, Z. Siu, R. Mahendiran, Solid State Commun. 150 (2010) 1670–1673.
[17] Y. Samancıoğlu, A. Coşkun, J. Alloys Compd. 507 (2010) 380–385.
[18] S.K. Barik, C. Krishnamoorthi, R. Mahendiran, J. Magn. Magn. Mater. 323 (2011) 1015–1021.
[19] Y. Sun, W. Tong, Y. Zhang, J. Magn. Magn. Mater. 232 (2001) 205–208.
[20] N. Chau, P.Q. Niem, H.N. Nhat, N.H. Luong, N.D. Tho, Physica B 327 (2003) 214–217.
[21] Md. A. Choudhury, S. Akther, D.L. Minh, N.D. Tho, N. Chau, J. Magn. Magn. Mater. 272 (2004) 1295–1297.
[22] E. Tka, K. Cherif, J. Dhahri, E. Dhahri, J. Alloys Compd. 509 (2011) 8047–8055.
[23] V.S. Amaral, J.S. Amaral, J. Magn. Magn. Mater. 272 (2004) 2104–2105.
[24] J.S. Amaral, M.S. Reis, V.S. Amaral, T.M. Mendonca, J.P. Araujo, M.A. Sà, P.B. Tavares, J.M. Vieira, J. Magn. Magn. Mater. 290 (2005) 686–689.
[25] S. Das, T.K. Dey, J. Phys. Condens. Matter. 18 (2006) 7629–7641.
[26] W.J. Lu, X. Luo, C.Y. Hao, W.H. Song, Y.P. Sun, J. Appl. Phys. 104 (2008) 113908–113914.
[27] S.K. Banerjee, Phys. Lett. 12 (1964) 16–21.
[28] D.N.H. Nam, N.V. Dai, L.V. Hong, N.X. Phuc, S.C. Yu, M. Tachibana, E. Takayama-Muromachi, J. Appl. Phys. 103 (2008) 043905–043909.
[29] W. Chen, W. Zhong, D.L. Hou, R.W. Gao, W.C. Feng, M.G. Zhu, Y.W. Du, J. Phys. Condens. Matter. 14 (2002) 11889–11896.
[30] P. Sande, L.E. Hueso, D.R. Miguens, J. Rivas, F. Rivadulla, M.A. Lopez-Quintela, Appl. Phys. Lett. 79 (2001) 2040–2042.
[31] V. Franco, J.S. Blázquez, A. Conde, Appl. Phys. Lett. 89 (2006) 222512–222515.
[32] A.N. Ulyanov, J.S. Kim, G.M. Shin, K.J. Song, Y.M. Kang, S.I. Yoo, Physica B 388 (2007) 16–19.
[33] N. Dhahri, A. Dhahri, K. Cherif, J. Dhahri, H. Belmabrouk, E. Dhahri, J. Alloys Compd. 507 (2010) 405–409.
[34] A.N. Ulyanov, J.S. Kim, G.M. Shin, Y.M. Kang, S.I. Yoo, J. Phys. D 40 (2007) 123–129.
[35] M.H. Phan, H.X. Peng, S.C. Yu, N.D. Tho, N. Chau, J. Magn. Magn. Mater. 285 (2005) 199–203.
[36] M.H. Phan, T.L. Phan, S.C. Yu, N.D. Tho, N. Chau, Phys. Status Solidi (B) 241 (2004) 1744–1747.
[37] V.K. Pecharsky, K.A. Gschneidner, A.O. Tsokol, Rep. Prog. Phys. 68 (2005) 1479–1539.
[38] V.K. Pecharsky, K.A. Gschneidner, Annu. Rev. Mater. Sci. 30 (2000) 387–429.
[39] M. Baazaoui, M. Boudard, S. Zemni, Mater. Lett. 65 (2011) 2093–2095.
[40] Z.M. Wang, G. Ni, Q.Y. Xu, H. Sang, Y.W. Du, J. Magn. Magn. Mater. 234 (2001) 371–374.
[41] J. Mira, J. Rivas, L.E. Hueso, F. Rivadulla, M.A. Lopez Quintela, J. Appl. Phys. 91 (2002) 8903–8905.